

1 **Supplementary Material**

2

3 **Hyperactivation of distinct thalamic nuclei
4 differentially impairs sleep physiology in rats**

5

6 Authors:

7 Joana Mendes Duarte¹*, Philipp Janz¹*, Andreas Bruns¹, Simon Gross¹, Marie Bainier¹,
8 Sébastien Debilly¹, Stephanie Schöppenthau¹, Thomas Bielser¹, Basil Künnecke¹, Jan M
9 Schulz¹, Roger L Redondo¹

10

11 1 Roche Pharma Research and Early Development, Roche Innovation Center Basel, F.
12 Hoffmann-La Roche AG, 4070 Basel, Switzerland.

13 * equal contributions

14

15

16

17

18

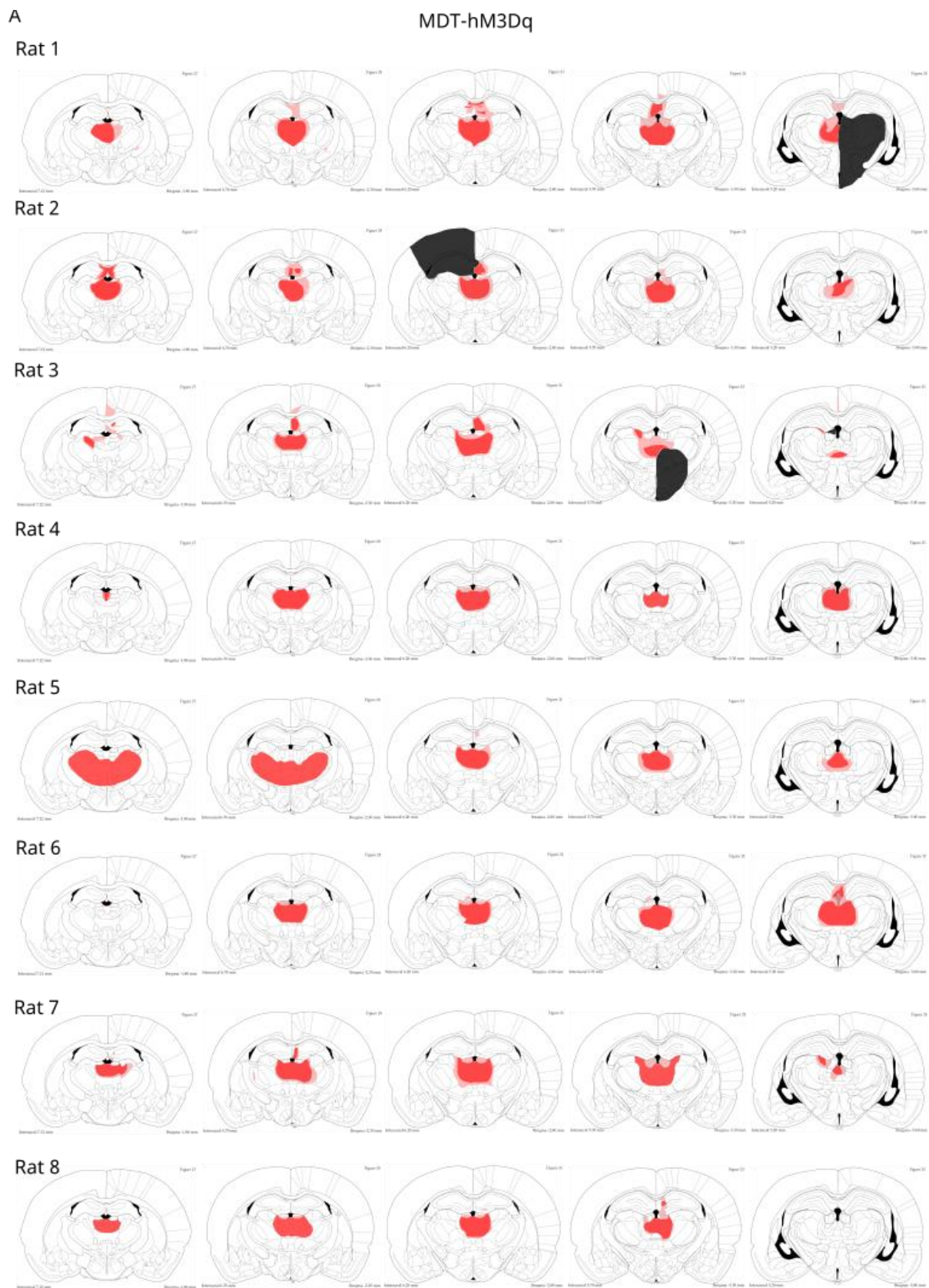
19

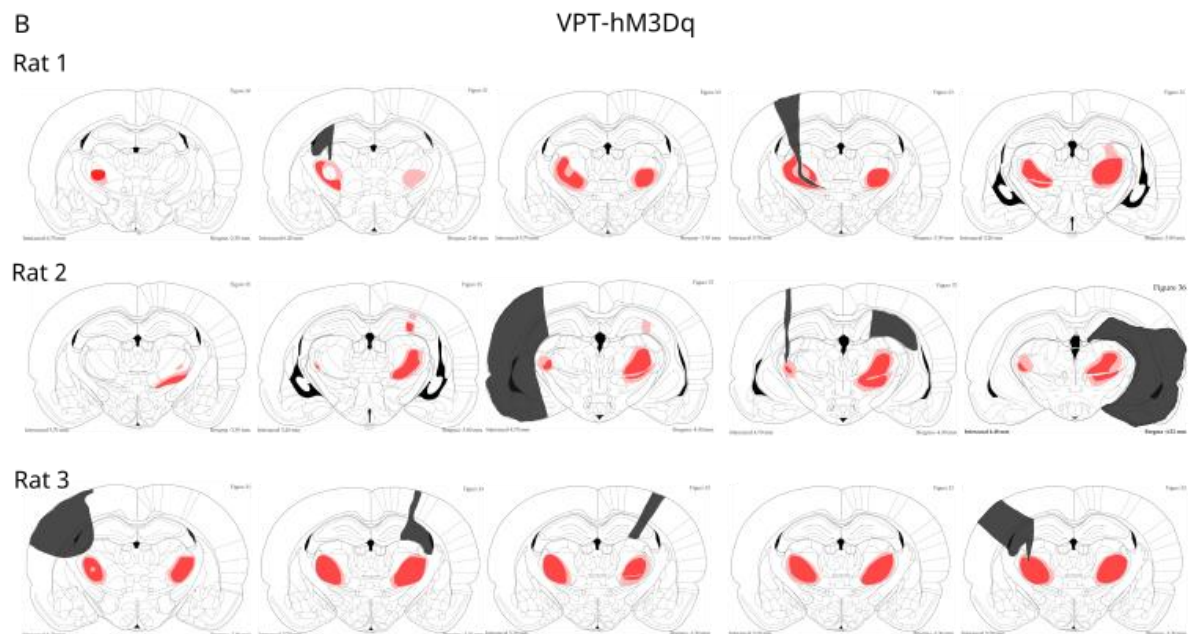
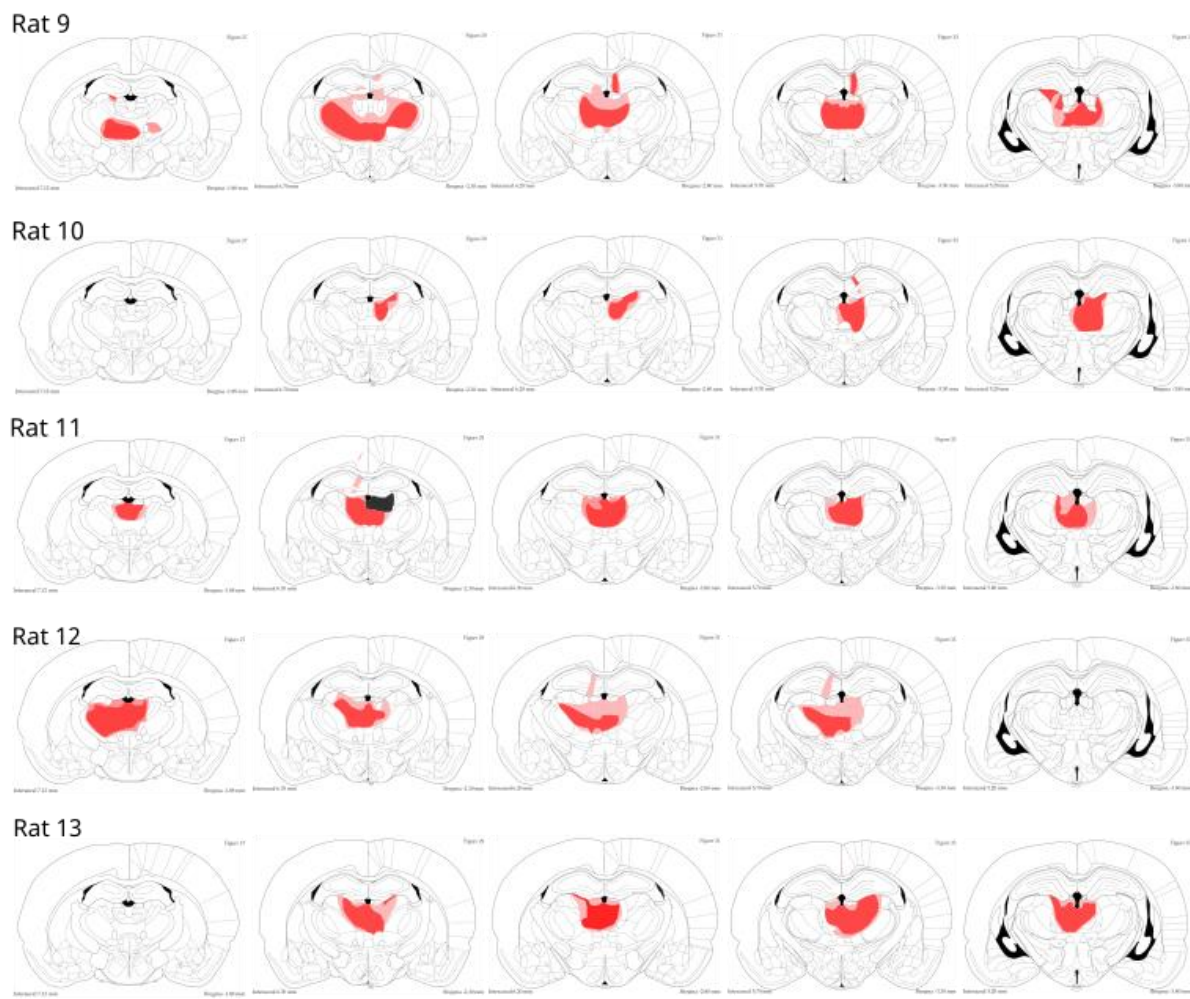
20

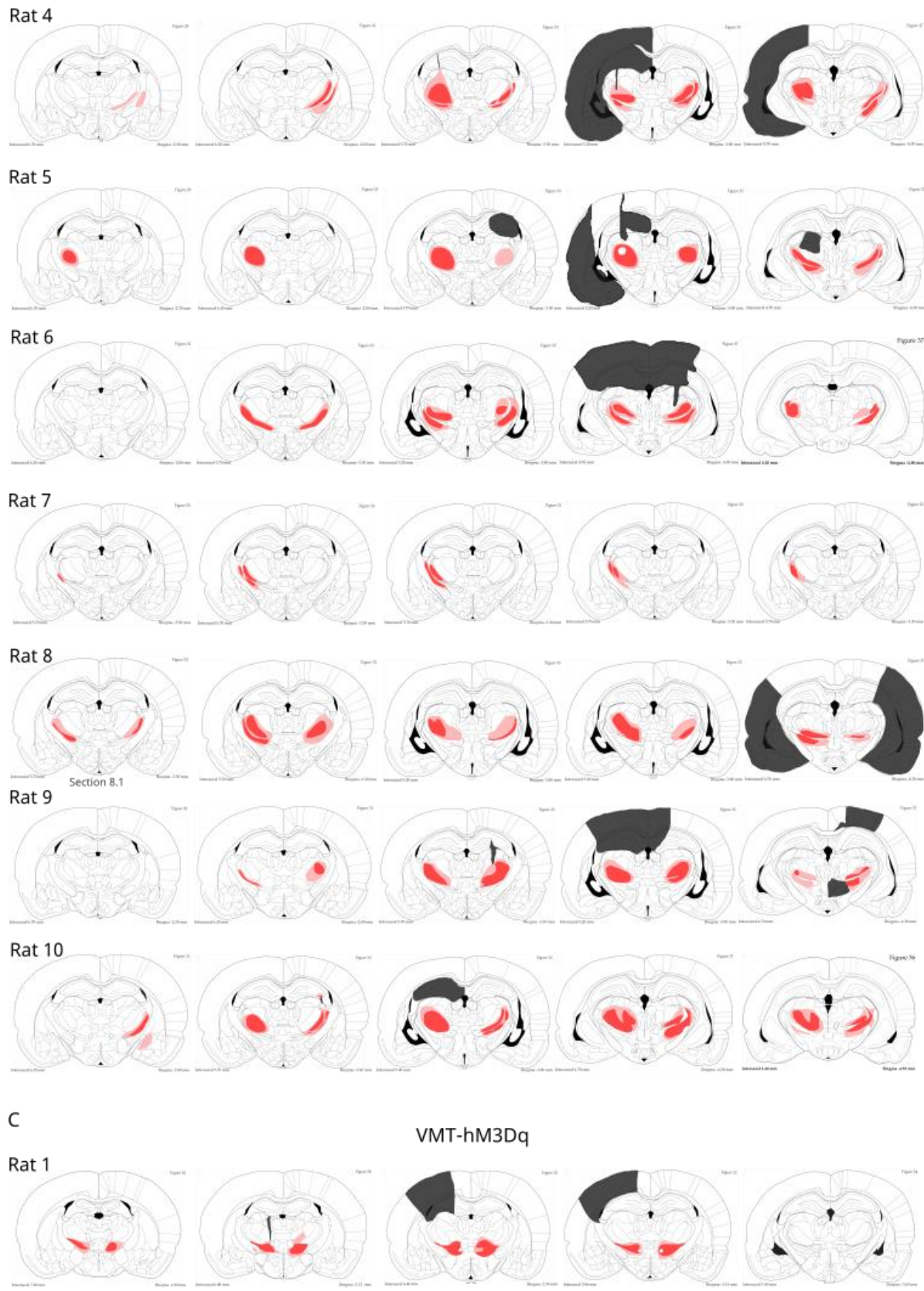
21

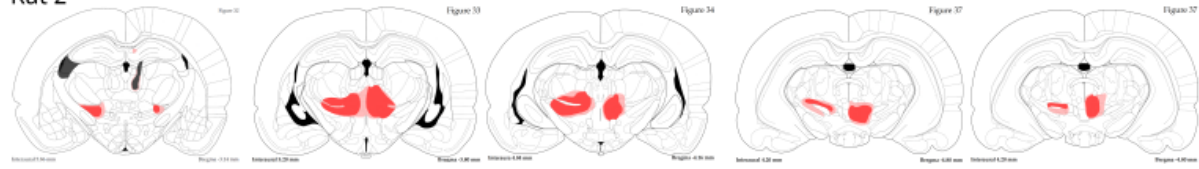
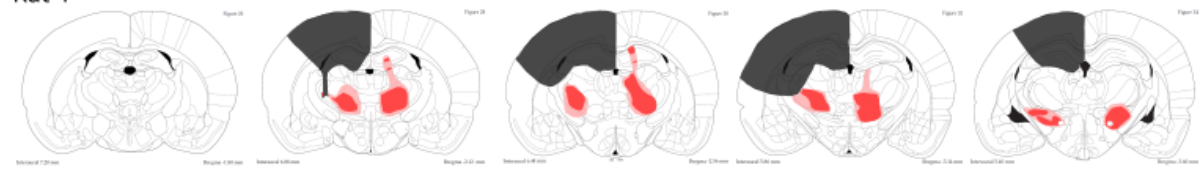
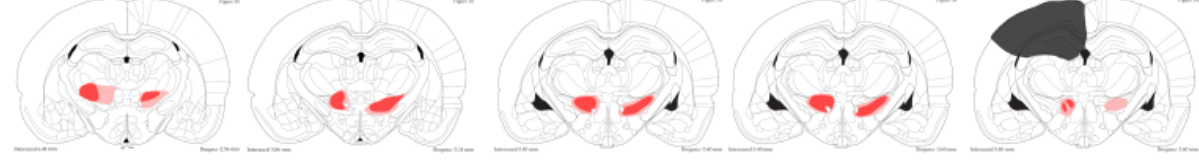
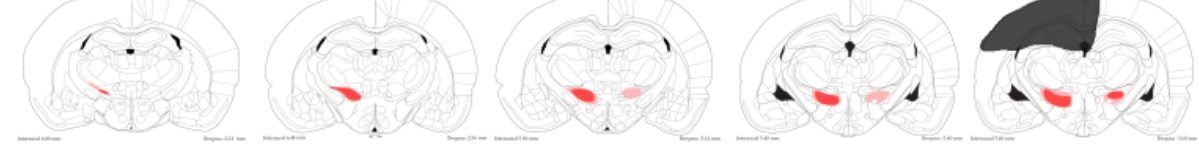
22

23







Rat 2**Rat 3****Rat 4****Rat 5****Rat 6****Rat 7****Rat 8****Rat 9**

29 **Supplementary Figure 1. Stereotactic targeting of MDT, VPT and VMT with AAV9-CaMKII α -
30 hM3D(Gq)_mCherry virus.**

31 (A) Corresponding coronal rat brain atlas images from Bregma level -2.30 to -4.30. MDT is highlighted in
32 red. (B) Images corresponding to the VPT-hM3Dq animals. (C) Images corresponding to the VMThM3Dq
33 animals.

34

35

36

37

38

39

40

41

42

43

44

45

46

47

48

49

50

51

52

53

54

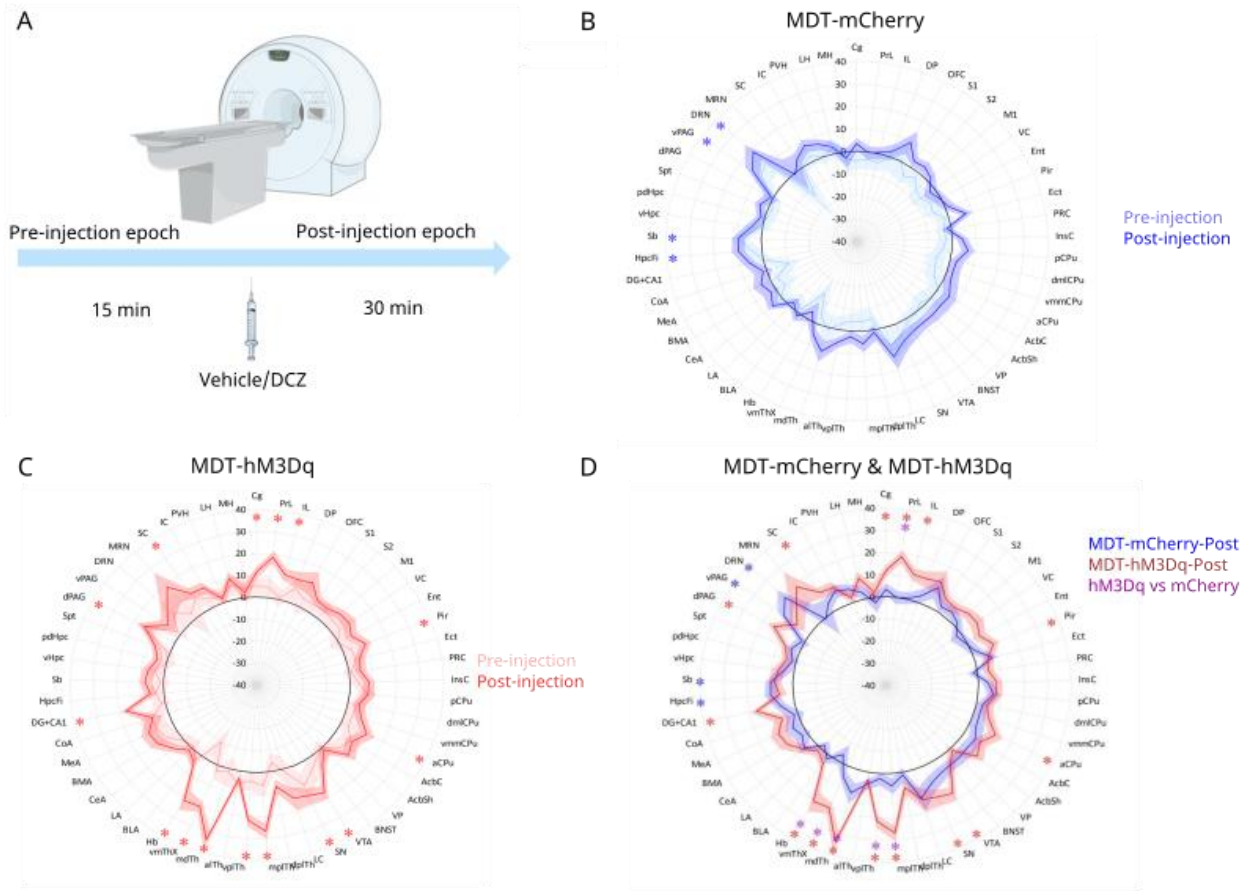
55

56

57

58

59



60

61 **Supplementary Figure 2. Perfusion-based MRI reveals distinct neuronal activation profiles**
62 **associated with MDT activation.** (A) Schematic of the experimental design and dosing scheme for the
63 chemogenetic manipulation. (B–D) Radar plots showing ROI-wise perfusion responses to DCZ treatment
64 in MDT-mCherry (blue) and MDT-hM3Dq (red) animals ($n=10$ per group) during the pre-injection (pale
65 colors) and the post-injection (dark colors) epochs, respectively. Response profiles (colored lines) are
66 shown as group-mean differences of the DCZ condition versus the vehicle condition (black circles at zero),
67 along with standard errors (shaded baNDDs/NPDs). Asterisks indicate modulations that are significant in
68 the sense of passing control of the false discovery rate (FDR) at 1%; blue and red asterisks refer to the
69 respective perfusion responses within each group, while purple asterisks highlight significant differences
70 between the responses of the two groups (interaction contrasts).

71 ROI abbreviations, in clockwise order: Cg: cingulate cortex, PrL: prelimbic cortex, IL: infralimbic cortex, DP:
72 dorsal peduncular cortex, OFC: orbitofrontal cortex, S1: primary SSC, S2: secondary SSC, M1: primary
73 motor cortex, VC: visual cortex, Ent: entorhinal cortex, Pir: piriform cortex, Ect: ectorhinal cortex, PRC:
74 perirhinal cortex, InsC: insula, pCPu: posterior CPu, dmlCPu: dorsomedial CPu, vmmCPu:
75 ventromedial CPu, aCPu: anterior CPu, AcbC: nucleus accumbens core, AcbSh: nucleus accumbens
76 shell, VP: ventral pallidum, BNST: bed nucleus of the stria terminalis, VTA: ventral tegmental area, SN:
77 substantia nigra, LC: locus coeruleus, dplTh: dorsal posterolateral thalamus, mplTh: medial posterolateral

78 thalamus, vPlTh: ventral posterolateral thalamus, aITh: anterolateral thalamus, mdTh: mediodorsal
79 thalamus, vMThX: other ventral nuclei of the mTh, Hb: habenula, BLA: basolateral amygdala, LA: lateral
80 amygdala, CeA: central amygdala, BMA: basomedial amygdala, MeA: medial amygdala, CoA: cortical
81 amygdala, DG+CA1: dentate gyrus & CA, HpcFi: fimbria hippocampi, Sb: subiculum, vHpc: ventral
82 hippocampus, pdHpc: posterior dorsal hippocampus, Spt: septal region, dPAG: dorsal PAG, vPAG: ventral
83 PAG, DRN: dorsal raphe nucleus, MRN: median raphe nucleus, SC: superior colliculus, IC: inferior
84 colliculus, PVH: paraventricular hypothalamic nucleus, LH: lateral hypothalamus, MH: median
85 hypothalamus

86

87

88

89

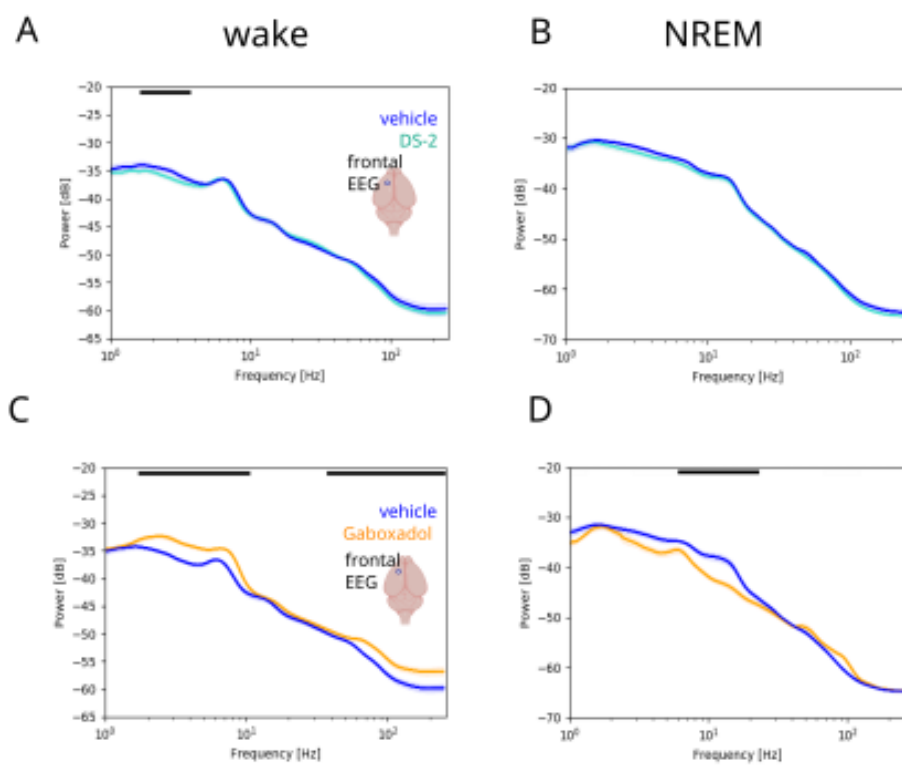
90

91

92

93

94



95 **Supplementary Figure 3. Effects of Gaboxadol and DS-2 in the absence of VMT activation.**

96 (A-B) Power spectral density plots during wake and NREM. for VMT-hM3Dq animals upon DS-2 or vehicle
97 administration (C-D) Power spectral density plots during wake and NREM. for VMT-hM3Dq animals upon
98 gaboxadol or vehicle administration.

99 Gaboxadol (15mg/kg) (orange); DS-2 (100 mg/kg) (cyan). N = 10 VMT-hM3Dq rats. Statistically significant
100 clusters ($p < 0.05$) are indicated as bars on top based on a paired cluster-based permutation test.

101

102

103

104

105

106

107

108 **Supplementary Methods**

109

110 **Pharmacological magnetic resonance imaging (phMRI).**

111

112 *Experimental design and procedure*

113 A total of 20 adult male Sprague-Dawley rats were used in this study, divided into two
114 experimental groups: control ($n=10$) and MDT-hM3Dq ($n=10$). Anesthesia of animals was
115 induced with isoflurane and maintained with medetomidine. Specifically, animals were
116 initially anesthetized with 4% isoflurane in oxygen-enriched air (40% O₂), delivered in an
117 inhalation chamber. Delivery was then continued at 1.2 l/min via a face mask at a lower
118 concentration of 2% for approx. 5 min and eventually at a maintenance concentration of
119 0.5% for the rest of the MRI session. In parallel to isoflurane reduction, subcutaneous
120 medetomidine (Dormilan[®]) administration was started with a bolus of 0.2 mg/kg (1 ml/kg),
121 followed by continuous infusion at 0.1 mg/kg/h (1 ml/kg/h). During the 5-minute
122 anesthesia transition phase, animals were positioned on a custom-made cradle, their
123 heads were immobilized in a stereotaxic frame with ear and bite bars, and an
124 ophthalmologic ointment was applied to their eyes to prevent drying. Anesthesia depth
125 was monitored through breathing rate (target: 60 breaths/minute) and O₂ and CO₂ levels

126 in inhaled and exhaled breathing gases using a PowerLab system (ADInstruments,
127 Spechnach, Germany). The body temperature was maintained at 37.5 °C with an electric
128 heating blanket in a feedback loop with a rectal thermometer. The total time under
129 anesthesia was approximately 90 min.

130 MRI was performed on a Biospec 7T / 20 cm horizontal-bore, small-animal MRI scanner
131 (Bruker BioSpin, Ettlingen, Germany) equipped with an actively decoupled 2-coil system
132 consisting of a body resonator for signal excitation and a head surface coil for reception.
133 Image acquisition was based on a standardized scan procedure. Briefly, following
134 localization of the most rostral extension of the corpus callosum as a landmark on scout
135 images, 8 coronal image planes were selected at +2.3, +1.0, −0.3, −1.6, −2.9, −5.3, −7.8,
136 and −10 mm from the bregma. All subsequent images were acquired in these planes, with
137 a field of view of 40 mm x 40 mm and a slice thickness of 1 mm. Firstly, a set of
138 T2-weighted fast spin-echo images (repetition time [TR]/effective echo time
139 $[TE_{eff}] = 2000 \text{ ms}/34 \text{ ms}$, acceleration factor 8, matrix 256 x 256 data points) was
140 obtained as an anatomical reference. Next, a T1-weighted image series required to
141 quantitate perfusion was obtained using an inversion-recovery gradient-echo sequence
142 with 8 inversion times (inversion time $[TI] = 21.7\text{--}1475.7 \text{ ms}$, TR/echo time
143 $[TE] = 3750 \text{ ms}/1.4 \text{ ms}$, matrix 128 x 64 data points). Finally, cerebral blood perfusion (as
144 a proxy of neuralactivity) was assessed by continuous arterial spin-labeling (CASL) with
145 centered-RARE readout ($TR/TE_{eff} = 3750 \text{ ms}/3.5 \text{ ms}$, acceleration factor = 64, matrix
146 128 x 128 data points, labeling pulse 2.5 s, postlabeling delay 0.4 s). 3 such CASL
147 volumes were acquired over a 12-minute epoch starting approx. 30 min after induction of
148 anesthesia (“pre-injection epoch”). After intraperitoneal injection of either vehicle or DCZ
149 (0.1 mg/kg) at approx. 50 min, a second and a third epoch with 3 CASL volumes each
150 were acquired, starting at approx. 55 min and 70 min, respectively (“post-injection
151 epochs”).

152

153 *Data processing and analysis*

154 MRI images were processed and analyzed using a Roche-developed software pipeline
155 implemented in MATLAB (The Mathworks; Natick, MA). In brief, structural (T2-weighted)
156 image volumes of each individual animal were spatially normalized to a Roche rat-brain

157 template using the open-source software SPM5 (Wellcome Trust Centre for
158 Neuroimaging, London, UK). Spatial normalization comprised a 12-parameter affine as
159 well as a nonlinear transform. The template was in alignment with a Roche digital atlas
160 delineating 53 predefined anatomical regions of interest (ROIs). T1-weighted and CASL
161 images were subjected to the spatial normalization transforms estimated from the
162 respective structural images and were then jointly processed to obtain maps of regional
163 blood perfusion, which was taken as a quantitative proxy for local neural activity.
164 Perfusion was averaged within each of the predefined ROIs and within each of the 3 12-
165 minute CASL epochs (across the 3 successive scans), yielding one scalar perfusion value
166 per animal (20), visit (2), ROI (53) and epoch (1 pre-, 2 post-injection). All image
167 reconstruction and processing steps prior to the statistical analysis were blind to
168 treatment. The statistical analysis as a final step did not include any further manipulation
169 of the data and thus excluded any expectation bias.

170

171 *Statistical analysis*

172 The statistical analysis of MRI data was performed in JMP Pro 17.2 (SAS Institute, Cary,
173 NC, USA). For each ROI, perfusion values were entered into a mixed model with *group*
174 (mCherry, hM3Dq) and *treatment sequence* (vehicle→DCZ, DCZ→vehicle) as fixed
175 between-subject effects, *treatment* (vehicle, DCZ) and *epoch* (pre-, post-injection) as
176 fixed within-subject effects and *subject* (animal) as random effect, plus all (also higher-
177 order) interactions among the fixed effects. While the *sequence* effect per se was not of
178 primary interest to us, it was important to factor it out (as it did actually interact with
179 *treatment* and to a lesser extent also with *group*treatment*), thereby increasing the
180 statistical sensitivity on the other effects. Within the framework of this model (i.e., based
181 on joint variance estimates), we formally tested the treatment effect (i.e., DCZ–vehicle, 2-
182 tailed) at pre-injection and at post-injection (both epochs jointly), in each group and as
183 interaction with group (hM3Dq–mCherry). Multiple testing was accounted for by
184 controlling the false discovery rate (FDR) at 1 % across the 6 contrasts and 53 ROIs,
185 using the Benjamini-Hochberg approach (Benjamini & Hochberg 1995). The specific
186 statistical tests applied to each analysis are detailed within the figure legends.

187

188

189

190